CHEMICAL ENGINEERING TRANSACTIONS
VOL. 32, 2013
A publication of AIDIC
The Italian Association of Chemical Engineering
Online at: www.aidic.it/cet
Chief Editors: Sauro Pierucci, Jiří J. Klemeš

ISBN 978-88-95608-23-5; **ISSN** 1974-9791
DOI: 10.3303/CET1332287

Temperature Effect on the Austenitic Stainless Steel UNS N08031 Used in the Wet Method Phosphoric Acid Production

Clara Escrivà-Cerdán[a], Encarna Blasco-Tamarit[a], Dionisio M. García-García[a], José García-Antón*[a], Abdellah Guenbour[b]

[a]Ingeniería Electroquímica y Corrosión (IEC). Departamento de Ingeniería Química y Nuclear. Universitat Politècnica de Valencia. Camino de Vera, s/n, 46022 Valencia, Spain.
[b]Laboratoire de Corrosion-Electrochimie, Faculté des Sciences, Université Mohammed V-Agdal, Rabat, Morocco.
jgarciaa@iqn.upv.es

The influence of temperature (between 20 and 80 ºC) on the electrochemical behaviour of UNS N08031 (Alloy 31) was evaluated in a contaminated phosphoric acid solution, which simulates the typical concentrations used in the industrial wet process (40 wt.% H_3PO_4, 2 wt.% H_2SO_4 and 0.42 wt.% KCl). Alloy 31 electrochemical behaviour was studied by means of polarisation curves and electrochemical impedance spectroscopy. Results demonstrated that temperature decreases the corrosion resistance of Alloy 31.

1. Introduction

The phosphoric industry has been always in centre of the attention because of severe environmental concerns (Seferlis et al., 2006; Klemeš, 2010; Bessarabov, 2012), however the aggressiveness of this environment can also cause severe corrosion problems in the industrial facilities. More than ninety-five per cent of phosphoric acid (H_3PO_4) is obtained by the wet process, in which the main stages involve the attack of phosphate ores by concentrated sulphuric acid (H_2SO_4 98%), filtration and concentration of phosphoric acid. This technique generates severe corrosion problems due to the presence of impurities such as chlorides, fluorides and sulphides. Although, depending on the nature of the phosphates and the type of phosphoric acid manufacturing process, the components of the equipment (reactors, agitators, pumps, drain, etc.) are subjected to slower or faster deterioration. The choice of materials used in this industrial process plays an important role since they must have both good chemical and mechanical resistance. These two characteristics are not always easy to obtain and a trade-off between these properties must be reached. In this sense, austenitic stainless steels are a good choice for phosphoric media. In this study, a highly alloyed austenitic stainless steel UNS N08031 (Alloy 31) was used.
The favourable effect of the alloying elements on the corrosion resistance is attributed to the formation of a protective passive surface film (Lee, 2006). This film is stable, invisible, thin, durable and extremely adherent and self-repairing and its stability depends on the nature of the corroding metal and ion present in the solution (Ibrahim et al., 2009).
The corrosion resistance of all types of austenitic stainless steel is based on the bilayer structure of the passive films formed spontaneously on their surface in aqueous solutions. These films act as a barrier layer, separating the metal's surface from the corrosive ions in the environment. Thus the understanding of the corrosion resistance of stainless steel lies in comprehending the properties of the passive films formed on the steel.
The aim of this work is to evaluate the influence of temperature on the electrochemical behaviour of Alloy 31 and the relative stability of the films formed on it.

Please cite this article as: Escriva-Cerdan C., Blasco-Tamarit M., Garcia-Garcia D.M., Garcia-Anton J., Guenbour A., 2013, Temperature effect on the austenitic stainless steel uns n08031 used in the wet method phosphoric acid production, Chemical Engineering Transactions, 32, 1717-1722 DOI: 10.3303/CET1332287

2. Experimental

2.1 Material, specimen preparation and solution

The material tested was the highly-alloyed austenitic stainless steel UNS N08031 (Alloy 31) provided by Thyssen Krupp VDM. The composition of this alloy (wt. %) is: 26.75 % Cr, 31.85 % Ni, 31.43 % Fe, 6.6 % Mo, 1.50 % Mn, 1.21 % Cu, 0.193 % N, 0.1 % Si, 0.005 % C, 0.002 % S, 0.017 % P. Alloy 31 electrodes were cylindrically shaped (8 mm in diameter and 55 mm long) and covered with a polytetrafluoroethylene (PTFE) coating. The area exposed to the solution was 0.5 cm^2.

The electrodes were abraded with wet emery paper of decreasing grit size (500 - 4000). After polishing, the samples were rinsed with distilled water and dried within a stream of air just before immersion.

The samples were tested in a polluted 40 wt.% phosphoric acid solution with 2 wt.% H_2SO_4 and 0.42 wt.% KCl, typical concentrations in the phosphoric acid industry (Becker, 1989).

2.2 Electrochemical tests

The electrochemical tests were performed in a conventional three-electrode cell, held at a constant temperature. A silver/silver chloride (Ag/AgCl) 3 M potassium chloride (KCl) electrode was used as a reference electrode and a platinum (Pt) wire as a counter electrode. The solution was deaerated by bubbling N_2 into the solution for 20 minutes before the test, and then the nitrogen atmosphere was maintained over the liquid surface during the duration of the test. The experiments were conducted under controlled temperature conditions at 20, 40, 60 and 80 ºC in order to study the influence of temperature on the corrosion behaviour of Alloy 31.

The anodic polarisation curves were measured by using a Solartron 1278 potentiostat. Before each polarisation measurement, the working electrodes were initially polarised in four steps from the OCP values to -0.4 $V_{Ag/AgCl}$. This potential was maintained for 1 hour in order to remove the passive film formed previously and to create reproducible initial conditions. Then the sample was polarised anodically from -0.4 $V_{Ag/AgCl}$ to the anodic direction at a scan rate of 0.1667 mV/s.

The electrochemical parameters estimated from these curves were: corrosion current density (i_{corr}) and corrosion potential (E_{corr}). In addition, transpassive potential (E_{tr}) was defined as the potential at which current density abruptly increases. The current density registered within the region before E_{tr} is almost constant which belongs to the passive current density (i_p). Therefore, all these parameters give information about general electrochemical behaviour of Alloy 31 in the contaminated H_3PO_4 solution.

On the other hand, electrochemical impedance spectroscopy (EIS) was used to study the passive films formed on Alloy 31. Prior to each EIS measurement, a passive potential of 0.5 $V_{Ag/AgCl}$ was applied to the sample for 1 h to allow for the growth of the passive film. EIS measurements were recorded in the range between 10^5 and 10^{-3} Hz with voltage amplitude of ± 5 mV, using an Autolab PGSTAT302N potentiostat.

3. Results and discussion

3.1 Potentiodynamic polarisation behaviour

Figure 1 shows the potentiodynamic polarisation curves for Alloy 31 in the contaminated phosphoric acid solution, which were obtained at 20, 40, 60 and 80 ºC to evaluate the effect of temperature on the general corrosion resistance of the stainless steel.

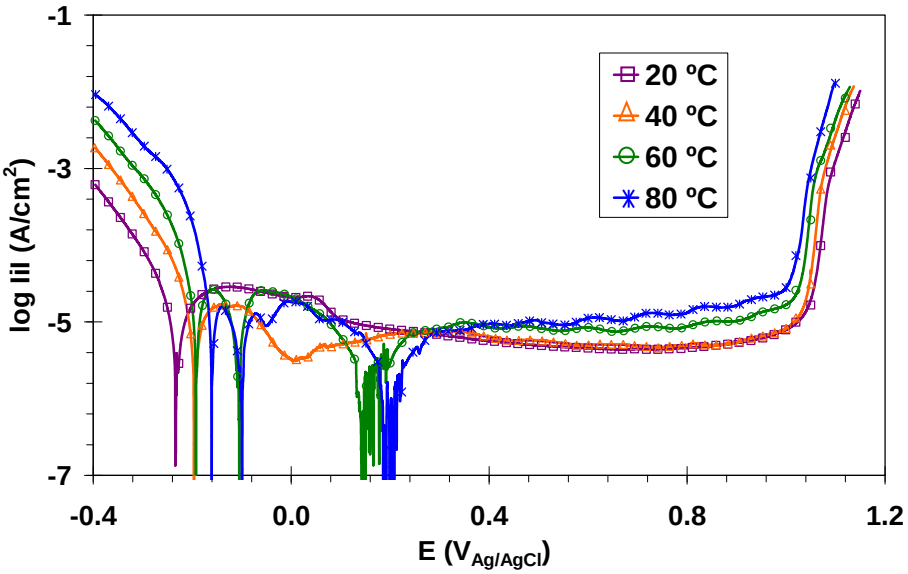

Figure 1: Potentiodynamic polarisation curves of Alloy 31 in 40 wt.% H_3PO_4 contaminated with 2 wt.% H_2SO_4 and 0.42 wt.% KCl at different temperatures.

The polarisation curves of Alloy 31 are similar at all temperatures, showing a very wide potential domain of passivity, generally in the potential range between 0.3 and 1 $V_{Ag/AgCl}$. Within this potential range, Alloy 31 registered a stable current density which increases with temperature. The transpassive potential E_{tr}, at which the breakdown of the passive film happened, shifted towards more active values as temperature increased.

Temperature clearly affects the cathodic reaction (Blasco-Tamarit et al., 2008) as it can be observed in the potentiodynamic curves, since the cathodic current densities increased with temperature (Figure 1). Temperature also favours the kinetics of the corrosion reactions, and especially the anodic dissolution of the metal, since the anodic current densities are higher as temperature increases.

The corrosion potentials (E_{corr}), corrosion current densities (i_{corr}), passive current density (i_p) and transpassive potential (E_{tr}) were obtained from the potentiodynamic polarisation curves and the numerical values are summarized in Table 1.

Table 1: Electrochemical parameters of Alloy 31 in the contaminated 40 wt.% H_3PO_4 solution at different temperatures after passive film formation at 0.5 $V_{Ag/AgCl}$.

T (ºC)	E_{corr} ($mV_{Ag/AgCl}$)	i_{corr} ($\mu A/cm^2$)	i_p ($\mu A/cm^2$)	E_{tr} ($mV_{Ag/AgCl}$)
20	-234	16.40	4.7	1029
40	-196	21.03	5.1	1017
60	143	2.82	8.7	1017
80	228	2.58	13.0	1006

E_{corr} and i_p increased with temperature, while i_{corr} did not present any clear trend with temperature. The increase of E_{corr} seems to be related to the higher cathodic current densities with temperature. The increase of i_p can be associated with the growth of the passive film which is enhanced with temperature. However, the transpassive potential, E_{tr}, decreased slightly due to the anodic dissolution of the metal which leads to a loss of passivity. In general, the effect of temperature in the contaminated solution is more significant due to the presence of aggressive ions which affect the anodic branch (Iken et al, 2007).

3.2 Electrochemical impedance behaviour

To investigate the influence of temperature on the relative stability of the passive films formed at 0.5 $V_{Ag/AgCl}$, EIS measurements were recorded after passive film generation at different temperatures. The impedance responses are presented in Nyquist and Bode formats in Figure 2.

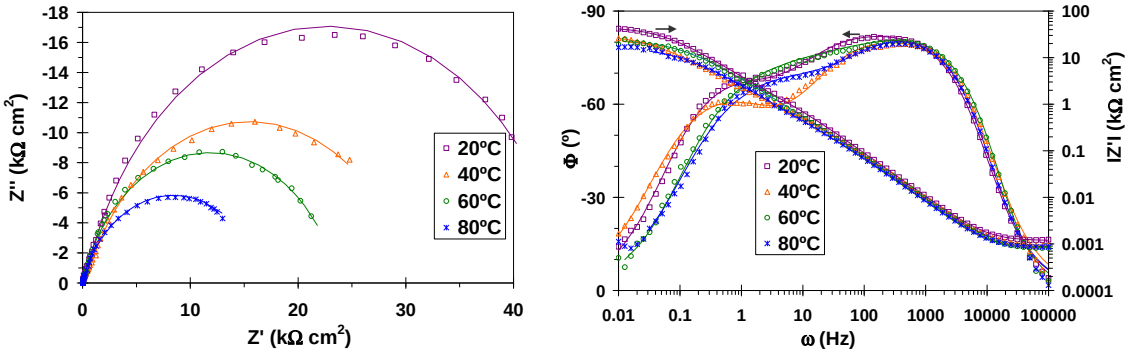

Figure 2: Nyquist diagrams (left) and Bode plots (right) of Alloy 31 after 1 h of immersion at 0.5 $V_{Ag/AgCl}$ in the contaminated H_3PO_4 solution with 2 wt.% H_2SO_4 and 0.42 wt.% KCl at different temperatures.

Impedance spectra present a somewhat unfinished capacitive arc which is temperature dependant, as evidenced by the overall decrease of the impedance values with temperature in the Nyquist diagrams. The smaller capacitive arcs as temperature increases indicate that the protective properties of passive films decrease. Moreover, Bode plots in Figure 2 depict two time constants, at high- and low-frequencies. This feature is often considered as the response of an inhomogeneous film composed of a compact inner layer and a less compact (porous) outer layer (Jüttner, 1990). According to this behaviour, a hierarchically distributed equivalent circuit (Figure 3) was used to simulate these results, as reported previously by Qiao et al., 2009.

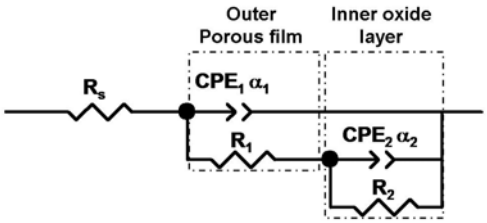

Figure 3: Equivalent electric circuit used to model the experimental EIS data with two hierarchically distributed time constants.

The modulus of the phase angle maxima is lower than 90º in all EIS spectra (Figure 2); this behaviour can be interpreted as a deviation from ideal capacitor behaviour due to the distribution of relaxation times as a consequence of heterogeneities on the electrode surface (Brug et al., 1984). Therefore, the use of a constant phase element (CPE) was necessary. The impedance of this element is defined by equation 1:

$$Z_{CPE} = \frac{1}{Q \cdot (j\omega)^{\alpha}} \qquad (1)$$

where Q is the CPE constant, ω is the angular frequency (rad/s), j^2=-1 is the imaginary number and α is the CPE exponent. Depending on α, CPE can represent resistance (α=0, Z_0=R), capacitance (α=1, Z_0=C), or Warburg impedance (α=0.5, Z_0=W).
The CPE elements, Q, have been converted into a pure capacitance (C) by means of the following equation:

$$C = \frac{(Q \cdot R)^{1/\alpha}}{R} \qquad (2)$$

The circuit represented in Figure 3 was used to explain the structure of the passive film formed on Alloy 31 in the contaminated phosphoric acid solution at 20, 40, 60 and 80 ºC. The quality of data fitting to the

equivalent circuit proposed was evaluated with the chi-squared values, which were lower than 10^{-3}, and the error percentages of the individual components of the equivalent circuit fitted. This is also shown in the diagrams of Figure 2, where the simulated data are shown as solid lines. The physical description of the model adopted in this work is that R_1, C_1 and R_2, C_2 refer to the resistance and capacitance of the outer porous layer and inner oxide layer.

The compact inner layer, known as barrier layer, is mainly composed of chromium oxides and is the major contributor. According to Reffass et al. 2009, the outer porous film is composed of iron phosphates, since in phosphoric acid media, phosphate species can precipitate with dissolved iron to form iron phosphates, which are characterized by a low solubility. In this situation, the outer layer is mainly a porous film of phosphates (Moraes et al., 2003).

The electrical parameters obtained by adjusting the experimental data show in Figure 2 are summarized in Table 2 as a function of temperature at the potential of 0.5 $V_{Ag/AgCl}$.

Table 2: Electrical parameters obtained by fitting the experimental results of EIS for Alloy 31 in the contaminated 40 wt.% H_3PO_4 solution at different temperatures after passive film formation at 0.5 $V_{Ag/AgCl}$.

T (ºC)	R_s (Ω cm^2)	R_1 (kΩ cm^2)	C_1 (μF·cm^{-2})	R_2 (kΩ cm^2)	C_2 (μF·cm^{-2})	R_P (kΩ cm^2)
20	1.18	1.48	21.36	83.21	47.19	84.69
40	0.89	1.03	25.02	59.79	148.82	60.83
60	0.86	0.76	26.78	23.89	65.22	24.65
80	0.86	0.37	23.93	16.84	66.43	17.21

According to the electrical parameters obtained, the resistance at very high frequencies corresponds to the resistance of the solution, R_s, which remains almost constant between 1.2 and 0.9 Ω cm^2 in all tests. The resistance of the inner oxide layer (R_2) is significantly larger than the values associated with the outer porous layer (R_1), which is consistent with the chosen physical model. These results indicate that the protection provided by the passive film was predominantly due to the barrier layer.

The values of R_1 indicate that the outer film can be considered as a thin and defective or porous film, as reported by Pan et al., 1998. It can be seen in Table 2 that R_1 decreases as temperature increases, which suggests that temperature favours the formation of a more porous film. This behaviour has been associated with the fact that at lower temperatures the outer porous layer is more stable as a result of the predominance of more stable phosphate iron compounds, resulting in a higher resistance (Escrivà-Cerdán et al., 2012). C_1 values are in the order of those expected to the double layer capacitance (Evgenij and Ros Macdonald, 2005) and hardly changes with temperature.

On the other hand, the parameters associated with the inner oxide film, R_2 and C_2 are more strongly affected by temperature. R_2 clearly decreases when temperature increases, which suggests that the films' electrical conductivity increases. The capacitance of the barrier layer, C_2, generally increases with temperature and this increase may indicate that the inner oxide film becomes thinner.

Finally, the sum of R_1 + R_2 is defined as polarisation resistance, R_P, and is related to the corrosion resistance of the metal. According to the results summarised in Table 2, R_P clearly decreases with temperature, indicating the worsening of the corrosion resistance of Alloy 31 in the contaminated phosphoric acid solution. In other words, temperature affects negatively the protective properties of the passive films formed on Alloy 31 at 0.5 $V_{Ag/AgCl}$.

4. Conclusions

The effect of temperature on the electrochemical behaviour of Alloy 31 was evaluated in a contaminated phosphoric acid solution, simulating typical concentrations in the wet process. The polarisation curves revealed that Alloy 31 exhibits a wide domain of passivity values indicating good protection efficiency.

The passive current density increased and the transpassive potential decreased as temperature increased, indicating a decrease in corrosion resistance with temperature.

EIS measurements showed that the protection provided by the passive film was predominantly due to the inner oxide film, while R_1 values demonstrated that the outer film can be considered as thin and porous. The influence of temperature was observed to affect more strongly the parameters associated with the inner oxide layer. The increase of temperature results in a higher electrical conductivity throughout the passive film, i.e. lower R_2 values. The higher capacitance values, C_2, may indicate a thinner oxide film.

The electrochemical results show that temperature negatively affects the protective properties of the passive films formed on Alloy 31 and, as a result, the corrosion resistance decreases with the increase of temperature.

Acknowledgements

Authors express their gratitude to the MAEC of Spain (PCI Mediterráneo C/8196/07, C/018046/08, D/023608/09 and D/030177/10) and to the Generalitat Valenciana (GV/2011/093) for the financial support and to Dra. Asunción Jaime for her translation assistance.

References

Becker P., 1989, Phosphates and phosphoric acid. Raw materials, technology, and economics of the wet process, Eds. M. Dekker, New York, USA.

Bessarabov, A., Zhekeyev, M.,Sandu, R., Kvasyuk, A., Stepanova, T., 2012, Chemical Engineering Transactions, 26, 513-518.

Blasco-Tamarit E., Igual-Muñoz A., García Antón J., García-García D., 2008, Effect of temperature on the corrosion resistance and pitting behaviour of Alloy 31 in LiBr solutions, Corros. Sci., 50, 1848-1857.

Brug G. J., Vandeneeden A. L. G., Sluytersrehbach M., Sluyters J. H., 1984, The analysis of alectrode impedances complicated by the presence of a constant phase element, J. Electroanal. Chem., 176, 275-295.

Escrivà-Cerdán C., Blasco-Tamarit E., García-García D.M., García-Antón J., Guenbour A., 2012, Effect of potential formation on the electrochemical behaviour of a highly alloyed austenitic stainless steel in contaminated phosphoric acid at different temperatures, Electrochim. Acta, 80, 248-256.

Evgenij B., Ros Macdonald J., 2005, Impedance Spectroscopy: Theory, Experiment and Applications, Ed. West Sussex, UK.

Ibrahim A.M.M, Abd El Rehim S.S., Hamza M.M., 2009, Corrosion behavior of some austenitic stainless steels in chloride environments, Mater. Chem. Phys., 115, 80-85.

Iken H., Basseguy R., Guenbour A., Bachir A. B., 2007, Classic and local analysis of corrosion behaviour of graphite and stainless steels in polluted phosphoric acid, Electrochim. Acta, 52, 2580-2587.

Jüttner K., 1990, Electrochemical impedance spectroscopy (EIS) of corrosion processes on inhomogeneous surfaces, Electrochim. Acta, 35, 1501-1508.

Klemeš, J.J., 2010, Environmental policy decision-making support tools and pollution reduction technologies: A summary, Clean Technologies and Environmental Policy, 12 (6), pp. 587-589.

Lee J.B., 2006, Effects of alloying elements, Cr, Mo and N on repassivation characteristics of stainless steels using the abrading electrode technique, Mater. Chem. Phys., 99, 224-234.

Moraes S. R., Huerta-Vilca D., Motheo A. J., 2003, Corrosion protection of stainless steel by polyaniline electrosynthesized from phosphate buffer solutions, Prog. Org. Coat., 48, 28-33.

Pan J., Leygraf C., Jargelius-Pettersson R. F. A., Linden J., 1998, Characterization of high-temperature oxide films on stainless steels by electrochemical-impedance spectroscopy, Oxid. Met., 50, 431-455.

Qiao Y. X., Zheng Y. G., Ke W., Okafor P. C., 2009, Electrochemical behaviour of high nitrogen stainless steel in acidic solutions, Corros. Sci., 51, 979-986.

Reffass M., Sabot R., Jeannin M., Berziou C., Refait P., 2009, Effects of phosphate species on localised corrosion of steel in $NaHCO_3$+NaCl electrolytes, Electrochim. Acta, 54, 4389-4396.

Seferlis, P., Klemeš, J., Bulatov, I., Koltsova, E., Kapustenko, P., Soboleva, I., 2006, Development of sustainable processes for waste utilisation in phosphoric acid industry. CHISA 2006 – 17th International Congress of Chemical and Process Engineering, Prague, Czech Republic, p.10.